BRODEA: An Efficient Brownian Dynamics Code Including Explicit Atoms

C. J. F. Solano

Jacobs University Bremen

Outline

Computational methods for studying substrate translocation

Molecular Dynamics (MD) + enhanced sampling methods

- Translocation is still out of reach of direct investigation using MD trajectories
- Enhance the sampling of a few crucial collective variables whose fluctuations are critical for the translocation by the introduction of a bias potential

Brownian Dynamics (BD)

- Dimensionality of the configurational space is reduced by projecting out the *uninteresting* degrees of freedom (solvent molecules)
- Environment is represented by a structureless dielectric medium

Outline

Main goal and general features

- Develop a fast and efficient software solution which enables us to study ion permeation and substrate translocation across a nanopore, i.e., artificial or biological channel, embedded in a bilayer membrane and surrounded by aqueous salt solutions
- System is divided into implicit and explicit or brownian particles
- The evolution for the cartesian coordinates of N brownian particles $\mathbf{r}^N = \{r_1, \ldots, r_{3N}\}$ is treated on a coarse time scale as a Markov process
- Implicit particles are described as a continuum dielectric (i.e., water molecules) or remained at fixed positions (i.e., implicit pore and membrane atoms)

Langevin equation and many-body PMF

- **Smoluchowski equation**

$$\left(\frac{\partial}{\partial t} - \hat{O}_{\mathbf{r}}\right) \rho(\mathbf{r}^N, t \mid \mathbf{r}_0^N, 0) = 0$$

  - $\rho(\mathbf{r}^N, t \mid \mathbf{r}_0^N, 0)$ is the conditional space probability distribution that the brownian particles adopt a configuration $\mathbf{r}^N \equiv \mathbf{r}^N(t)$ at time t given the initial configuration $\mathbf{r}_0^N \equiv \mathbf{r}^N(0)$ at time $t = 0$
  - The Smoluchowski operator $\hat{O}_{\mathbf{r}} = \sum_i^{3N} \frac{\partial}{\partial r_i} D_i \left(\frac{\partial}{\partial r_i} - \beta r_i\right)$ acts on the variables $\mathbf{r}^N$, where β is the inverse of thermal energy and D_i is the self-diffusion constant of the brownian particle associated with index i
  - Analogue of the Liouville equation in the all-atom description

- **Langevin equation**

$$\frac{dr_i}{dt} = \left[\beta D_i(\mathbf{r}^N) f_i(\mathbf{r}^N) + \frac{\partial}{\partial r_i} D_i(\mathbf{r}^N)\right] + \sqrt{2D_i(\mathbf{r}^N)}\eta_i(t)$$

  - $f_i = -\frac{\partial}{\partial r_i} W(\mathbf{r}^N)$ is the force acting in direction i and $W(\mathbf{r}^N)$ is the many-body PMF
  - η_i is a gaussian white noise process

Langevin equation and many-body PMF

- **Many-body PMF**

$$
\begin{aligned}
W(\mathbf{r}^N) = & \sum_{bonds} K_b(b-b_0)^2 + \sum_{angles} K_\theta(\theta-\theta_0)^2 + \sum_{Urey-Bradley} K_S(S-S_0)^2 \\
& + \sum_{dihedrals} K_\varphi(1+\cos(n\varphi-\delta)) + \sum_{impropers} K_\omega(\omega-\omega_0)^2 \\
& + \sum_{residues} U_{CMAP} + \sum_{\alpha}^{N} \left\{ q_\alpha \left[\phi_{sf}(\mathbf{r}_\alpha) + \frac{\phi_{rf}(\mathbf{r}_\alpha)}{2} \right] + U_{core}(\mathbf{r}_\alpha) \right\} \\
& + \sum_{\beta>\alpha}^{N} 4\epsilon_{\alpha\beta} \left[\left(\frac{\sigma_{\alpha\beta}}{r_{\alpha\beta}} \right)^{12} - \left(\frac{\sigma_{\alpha\beta}}{r_{\alpha\beta}} \right)^{6} \right] + w_{sr}(r_{\alpha\beta}) + \frac{q_\alpha q_\beta}{4\pi\varepsilon_0\varepsilon(r_{\alpha\beta})r_{\alpha\beta}}
\end{aligned}
$$

Outline

Nonbonded list

- BRODEA use finite cutoffs to reduce the number of nonbonded interactions
- The calculation to determine which particle pairs fall within the cutoff distance can be time-consuming
- Verlet idea: reduce the frequency of this calculation by extending the spherical cutoff region about each particle with an additional volume shell
- Between consecutive BD steps particle positions do not change drastically. Therefore, the same nonbonded list can be used for several BD steps

Numerical integration of Langevin equations

- **Euler-Maruyama method**

$$r_i(t+\Delta t) = r_i(t) + \beta D_i(\boldsymbol{r}^N(t)) f_i(\boldsymbol{r}^N(t))\Delta t + \frac{\partial D_i(\boldsymbol{r}^N(t))}{\partial r_i}\Delta t + \sqrt{2D_i(\boldsymbol{r}^N(t))\Delta t}Z(t)$$

where Δt is the time step and $Z(t)$ is a standard normal random variable

- **Milstein method**

$$r_i(t+\Delta t) = r_i(t) + \beta D_i(\boldsymbol{r}^N(t)) f_i(\boldsymbol{r}^N(t))\Delta t + \frac{1}{2}\frac{\partial D_i(\boldsymbol{r}^N(t))}{\partial r_i}\Delta t\left[(Z(t))^2+1\right] + \sqrt{2D_i(\boldsymbol{r}^N(t))\Delta t}Z(t)$$

Numerical integration of Langevin equations

- **Predictor-corrector method**
  - **Predictor step**

$$\tilde{r}_i(t+\Delta t) = r_i(t) + \beta D_i(\boldsymbol{r}^N(t)) f_i(\boldsymbol{r}^N(t))\Delta t + \frac{\partial D_i(\boldsymbol{r}^N(t))}{r_i}\Delta t + \sqrt{2D_i(\boldsymbol{r}^N(t))\Delta t}Z(t)$$

  - **Corrector step**

$$\begin{aligned} r_i(t+\Delta t) = r_i(t) &+ \frac{\beta}{2}\left[D_i(\boldsymbol{r}^N(t))f_i(\boldsymbol{r}^N(t)) + D_i(\tilde{\boldsymbol{r}}^N(t+\Delta t))f_i(\tilde{\boldsymbol{r}}^N(t+\Delta t))\right]\Delta t \\ &+ \frac{1}{4}\left[\frac{\partial}{\partial r_i}D_i(\boldsymbol{r}^N(t)) + \frac{\partial}{\partial r_i}D_i(\tilde{\boldsymbol{r}}^N(t+\Delta t))\right]\Delta t \\ &+ \frac{\sqrt{2D_i(\boldsymbol{r}^N(t))\Delta t} + \sqrt{2D_i(\tilde{\boldsymbol{r}}^N(t+\Delta t))\Delta t}}{2}Z(t) \end{aligned}$$

Constraints and constant electric field approach

- **Holonomic bond distance constraints**
  - **SHAKE** algorithm
  - **LINCS** algorithm (easily parallelizable)
- **Harmonic restraints** on selected atoms or C_α atoms
- **Constant external electric field**
  - A simple approach to implement a transmembrane potential
  - A constant electric field E is applied along the channel axis
  - E drives a voltage difference over the whole system $V = EL$, where L is the length of the simulation box along the channel axis

Boundary conditions

- **Grand canonical Monte Carlo (GCMC) algorithm**
  - GCMC allows fluctuations in the number of ions
  - Particle creation and destruction is accepted based on the energy of the system and the chemical potential of the ion species
  - Unphysical creation and destruction is restricted to control cells (CCs) defined in the boundaries of the simulation box
  - Time consuming
- **Periodic boundary conditions (PBCs)**
  - PBCs are conceptually simpler, involve less calculations, and are considerably faster at moderate and high ion concentrations
  - The size of the system has to be adjusted to contain an integer number of ions
  - PBCs allows for only modeling symmetric solutions at each side of the channel
- **Particle counting (PACO) algorithm**
  - Ions are inserted into and deleted from the CCs only when need
  - PACO needs only ion counting inside the CCs without the computationally expensive energy calculation

Simulations schemes

Table : Simulations schemes available in BRODEA code where system boundaries and the methods for estimating the static field ϕ_{sf} are highlighted. Key: eq: equilibrium, noneq: nonequilibirum; P: Poisson equation, PB-V: modified Poisson-Boltzmann equation including transmembrane potential, Efiled: constant electric field

Scheme	Condition	System boundaries	Static field
eGCMC/BD	eq	GCMC	PB
GCMC/BD	noneq	GCMC	PB-V
eBD	eq	PBCs	P
BD	noneq	PBCs	P + Efield
ePACO/BD	eq	PACO	P
PACO/BD	noneq	PACO	P + Efield

Outline

Ion permeation across OmpC pore

Figure : (A) Surface representation of the OmpC trimer (PDB ID: 2J1N) from *E. coli* with each monomer formed by 16 β-strands. (B) An OmpC monomer is shown with the L3 loop in yellow leading to a narrow pore together with important negatively charged residues (D105, E109 and D113) shown as sticks. (C) Positively charged residues (K16, R37, R74 and R124) located on the barrel wall, opposite to L3 loop, are shown as sticks

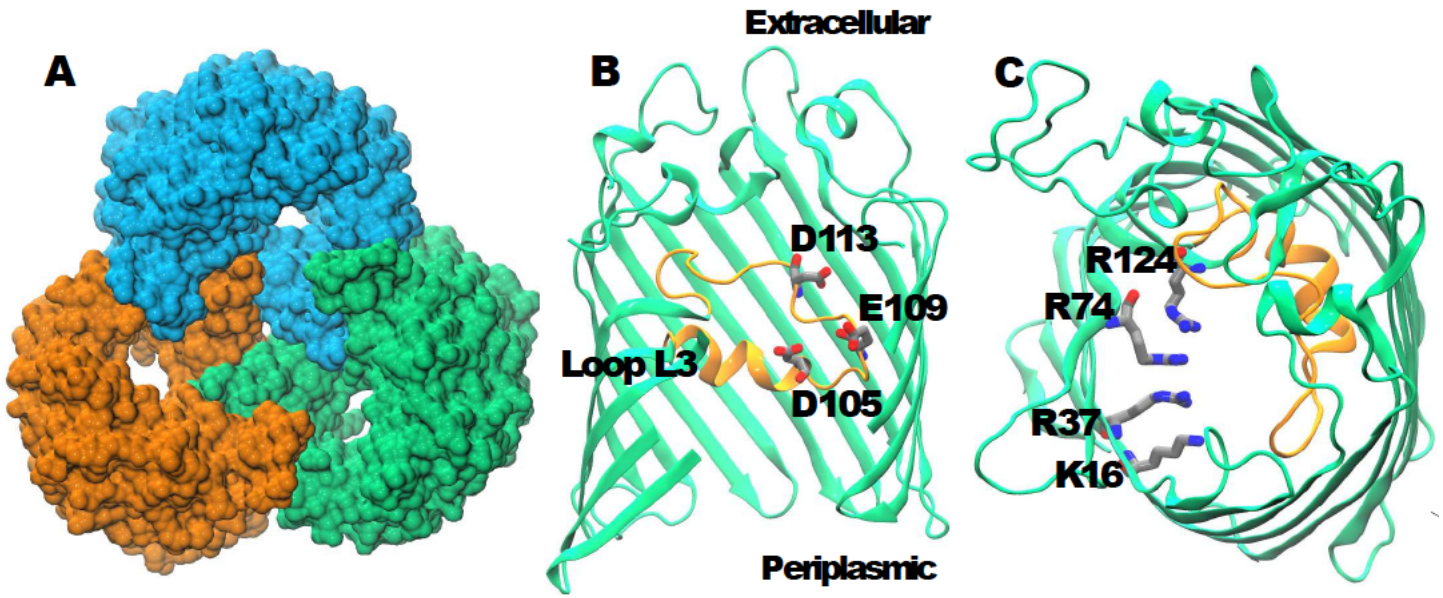

- Residues from 104 to 114 in the L3 loop (including negatively charged D105, E109 and D113) undergo thermal fluctuations
- Positively charged residues K16, R37, R74 and R124 also undergo thermal fluctuations

Ion permeation across OmpC pore

Table : Average number of ions in the channel N and average conductance G for 0.3 M KCl at 0.1 V transmembrane potential and 300 K. Simulation time is 100 ns for each independent run

SCHEME	BD PROP.	CONSTR.	N_{K+}	N_{Cl-}	G [nS]	CPU TIME [hours]
GCMC/BD (old)	EM	SHAKE	7.68±0.20	1.33±0.20	0.73±0.21	155.59±3.86
GCMC/BD	EM	SHAKE	7.51±0.15	1.28±0.15	0.70±0.27	34.21±0.47
GCMC/BD	EM	LINCS	7.75±0.34	1.42±0.30	0.81±0.17	33.62±0.17
BD	EM	SHAKE	7.42±0.47	0.91±0.46	0.63±0.26	24.18±0.25
BD	EM	LINCS	7.63±0.45	1.08±0.46	0.72±0.20	24.00±0.20
PACO/BD	EM	SHAKE	7.93±0.42	1.50±0.46	0.78±0.26	47.68±0.54
PACO/BD	EM	LINCS	7.75±0.42	1.37±0.37	0.68±0.25	52.83±3.55
GCMC/BD	MLS	SHAKE	7.42±0.25	1.14±0.22	0.66±0.17	33.90±0.79
GCMC/BD	MLS	LINCS	7.56±0.29	1.35±0.33	0.61±0.19	33.98±0.78
BD	MLS	SHAKE	7.77±0.33	1.29±0.41	0.69±0.21	24.17±0.23
BD	MLS	LINCS	7.70±0.44	1.24±0.39	0.68±0.21	24.04±0.16
PACO/BD	MLS	SHAKE	7.58±0.47	1.25±0.46	0.62±0.19	47.71±0.51
PACO/BD	MLS	LINCS	7.73±0.41	1.32±0.49	0.73±0.29	47.97±0.76
GCMC/BD (old)	PC	SHAKE	6.59±0.20	0.79±0.23	0.63±0.14	154.88±1.18
GCMC/BD	PC	SHAKE	7.53±0.38	1.41±0.38	0.60±0.14	52.81±0.44
GCMC/BD	PC	LINCS	7.51±0.26	1.31±0.33	0.69±0.19	53.00±0.65
BD	PC	SHAKE	7.81±0.43	1.38±0.42	0.79±0.23	42.96±0.28
BD	PC	LINCS	7.61±0.40	1.11±0.44	0.62±0.27	43.92±0.74
PACO/BD	PC	SHAKE	7.64±0.61	1.33±0.66	0.67±0.23	69.66±0.92
PACO/BD	PC	LINCS	7.82±0.36	1.49±0.37	0.71±0.22	68.74±0.64
applied-field MD			5.95±1.64	1.87±1.06		
Experiment [3]					∼0.41	

[3] I. Biro *et al*, *Biophys. J.* **97**, 1898 (2009)

Ion permeation across OmpC pore

Figure : 1D multi-ion average PMF for 0.3 M KCl solution under equilibrium conditions (i.e., zero transmembrane potential) and 300 K. The results for the K^+ ions are represented in red while the $Cl-$ ions are in green. A different line type is used for each different scheme

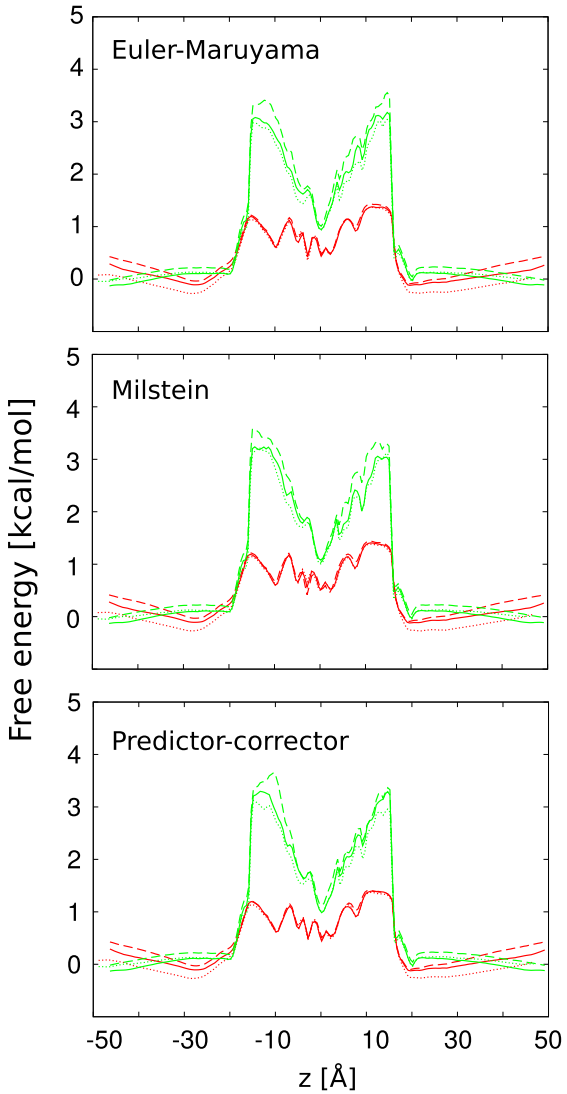

Outline

Future work

- Apply BRODEA for ion permeation using a more realistic OmpC representation and compare with MD results
- Implement an alternative protocol in which all interactions are treated at the forces field level
- Apply BRODEA for antibiotic translocation